Journal of Molecular Liquids 326 (2021) 115286

Contents lists available at ScienceDirect

Journal of Molecular Liquids

journal homepage: www.elsevier.com/locate/molliq

Magnetic field effects on O_2/Ar liquid flow through a platinum micro-channel via dissipative particle molecular dynamics approach

Abdolmajid Taghipour, Arash Karimipour *, Masoud Afrand, Somaye Yaghoubi, Mohammad Akbari

Department of Mechanical Engineering, Najafabad Branch, Islamic Azad University, Najafabad, Iran

ARTICLE INFO

Article history:
Received 10 December 2020
Received in revised form 25 December 2020
Accepted 31 December 2020
Available online 06 January 2021

Keywords:
Dissipative particle dynamics
Fluid
Argon
Oxygen
Platinum
Micro-channel

ABSTRACT

In this computational work, we describe atomic behavior of Ar and O_2 fluids in Pt micro-channel with external magnetic field. Our Dissipative Particle Dynamics (DPD) simulation results show the poiseuille flow for these structures with/without external magnetic field. These DPD simulations done with LAMMPS (Large scale Atomic/Molecular Massively Parallel Simulator) package. Numerically, maximum value for density of Ar/O_2 particles in platinum micro-channels is 0.042/0.043. Further, maximum ratio of these particles velocity reach to 0.104/0.097. This maximum value occur in middle region of micro-channel. Temperature of various fluid particles varies with similar behavior and reach to maximum value in 390/489 simulated bins of DPD box. Finally, we expected these computational results can be used for optimize the industrial process such as mass and heat transfer.

1. Introduction

In physics, a fluid is a substance that continually deforms (flows) under an applied external force which implemented with outer sources such as electric or magnetic field. The behavior of fluids at the micro-scale can differ from macro-scale. In recent years, researches done to describes how these structures behaviors change, and how they can be worked around, or exploited for new uses [1–5]. In practical cases, fluid particles controlling is an important process for using of this atomic structures to industrial applications. Micro-channels is one promising methods which used in fluid control and heat transfer procedures. Micro-channel in micro-technology is a channel with a hydraulic diameter below 1 mm size [6,7]. Technically, micro-fluids designing one of the excellent methods to fluids controlling. Micro-fluid designing refers to the behavior, precise control, and manipulation of fluids that are geometrically constrained to a small scale at which surface forces dominate volumetric forces [8]. Historically, Micro-fluid designing emerged in the beginning of the 1980s and is used in the development of inkjet printheads, DNA chips, lab-on-a-chip technology, micro-propulsion, and micro-thermal technologies [9]. Computational methods is one of the various approaches to particles (such as atoms and molecules) study [10–14]. Computational methods described fluids behavior appropriately [15–20]. Dissipative particle dynamics (DPD) method, is a computer simulation for study of micro-scale phenomena [21–23]. Coarse graining modeling used in this approach which leads to an inter particle force implementing for various structures [24–26]. Theoretically, Fokker–Planck equation solved in DPD simulations which this process cause to predict the continuum phenomena by using this method. In previous work, this computational method has been used for study of various fluids. In previous works, DPD method used successfully for fluid study. Xu et al. [27] showed the DPD method widely used in predicting the channel flow containing various soft matter systems. The general aspect and basic formulations of DPD are introduced in this work, and different boundary conditions are presented for wall-bounded flows. In addition, the models based on DPD developed to simulate flow-induced transport through fluidic channels for some typical soft matter systems are discussed, including red blood cells, vesicles, polymers, and bio-macromolecules. Abu-Nada et al. [28] introduce a two-component DPD model to investigate heat transfer enhancement in natural convection using Al_2O_3-water nano-fluid. This DPD model used two different types of particles to represent the base fluid particles and the nanoparticles. This work results revealed that for the case of low Rayleigh numbers some enhancements were observed using low volume fraction of nanoparticles, however further increase in volume fraction of nanoparticles caused a deterioration in heat transfer. Tong et al. [29] used extended energy-conserving dissipative particle dynamics (eDPD) to investigate the macromolecule behaviors as well as the flow of macromolecular suspension confined in a micro-channel under thermal gradient. The results show that the thermal gradient effect on the macromolecular suspension flow is significant, and the macromolecules are more prone to reach an extended stretching state as the

* Corresponding author.
E-mail address: arashkarimipour@gmail.com (A. Karimipour).

https://doi.org/10.1016/j.molliq.2021.115286
0167-7322/

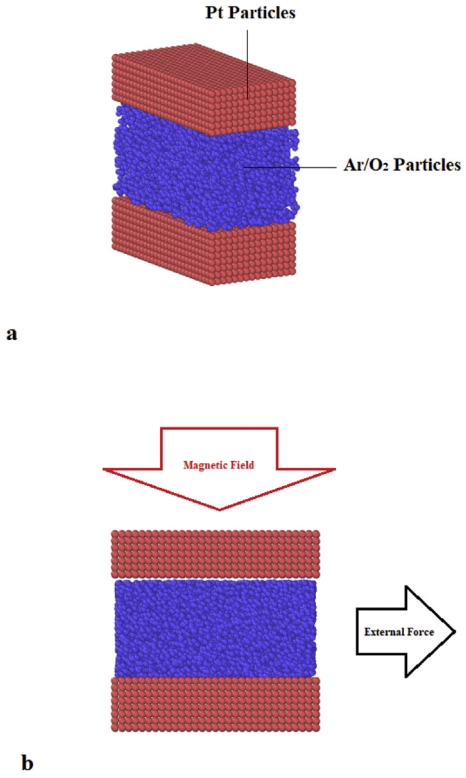

Fig. 1. Ar/O_2 fluid and Pt micro-channel arrangement in our computational work: a) without external magnetic field and b) with external magnetic field.

temperature becomes higher. Mai-Duy et al. [30] calculated the viscosity of the solvent phase is typically estimated by a DPD approach, where the fluid is subjected to a flow process, and the local stress and shear rate tensors. Results show that, the obtained values in this study (shear stress/shear rate) can be used in calculating the particulate fluid rheology appropriately. In this work we use DPD simulations to simulate atomic behavior of Ar and O_2 fluids in Pt micro-channel in presence of external magnetic field.

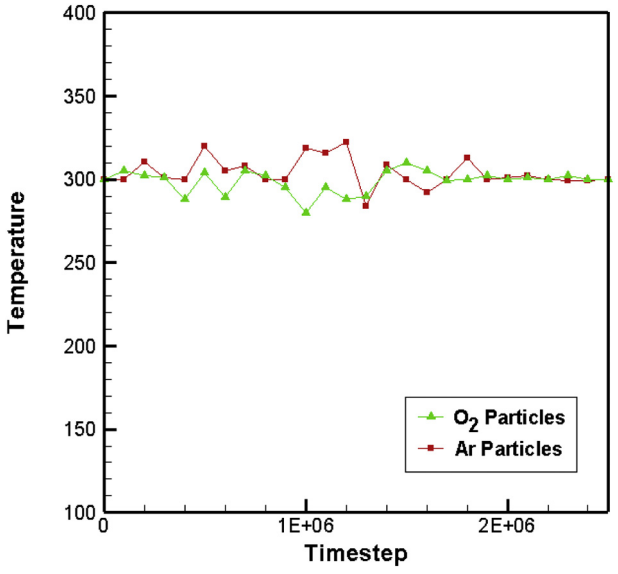

Fig. 2. Temperature fluctuation of O_2/Ar fluid in Pt micro-channel as a function of time steps.

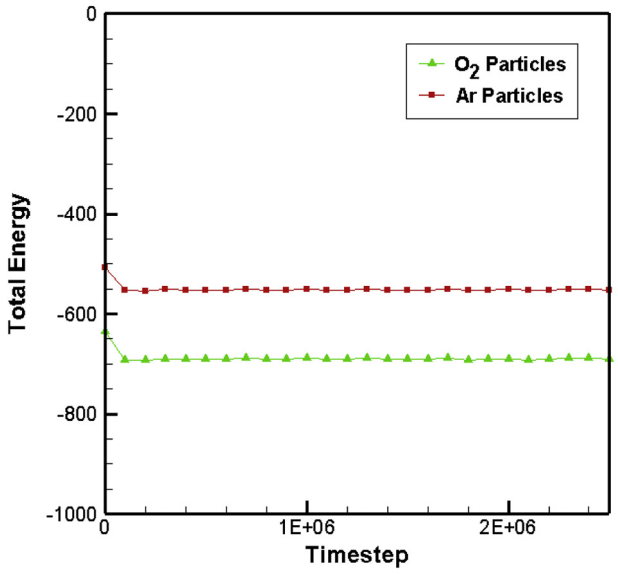

Fig. 3. Total energy variation of Ar/O_2 fluid in Pt micro-channel as a function of time steps.

2. Computational method

In this computational work, we use DPD method to describe the Ar/O_2 atomic behavior in presence of time dependent external magnetic field. Historically, this method propose for the first time by Hoogerbrugge and Koelman [31,32]. They suggested an effective method for designing micro-channels in the laminar and fully developed flow. Later, espanol improved this computational approach to ensure the appropriate equilibrium state [33]. Today, various DPD approaches with optimized computational complexity and good control of transport properties are released [34]. Technically, DPD is a coarse-grained version of molecular dynamics and emerged as a simple yet potentially powerful alternative for mesoscopic simulations. In this method, each DPD particle represents a cluster of actual molecules of the flow field. Each particle interacts with surrounding particles through a set of distance and velocity dependent forces within a certain cutoff radius. In this method, sum of the forces applied to the particle "I" is shown by following relation [31–34]:

$$F_i = \sum_{j \neq i} \left(F_{ij}^C + F_{ij}^D + F_{ij}^R \right) \quad (1)$$

where, F_{ij}^C is a conservative force, F_{ij}^D is a dissipative force and F_{ij}^R is a random force, respectively. All used parameters in the force equation are dimensionless. These interaction forces defined as below [31,32]:

$$F^C = A\omega(r) \quad (2)$$

$$F^D = -\gamma\omega^2(r)(\mathbf{r_{ij}}.\mathbf{v_{ij}}) \quad (3)$$

$$F^R = \sigma\,\omega(r)\alpha\,(\Delta t)^{-1/2} \quad (4)$$

$$\omega(r) = 1 - r/r_c \quad (5)$$

Table 1
Total energy temperature and value of Ar/O_2 fluid in Pt micro-channel after 2,500,000 time step.

Fluid Type	Temperature (Unit Less)	Total Energy (Unit Less)
Ar particles	299.98	−551
O_2 particles	300.05	−690

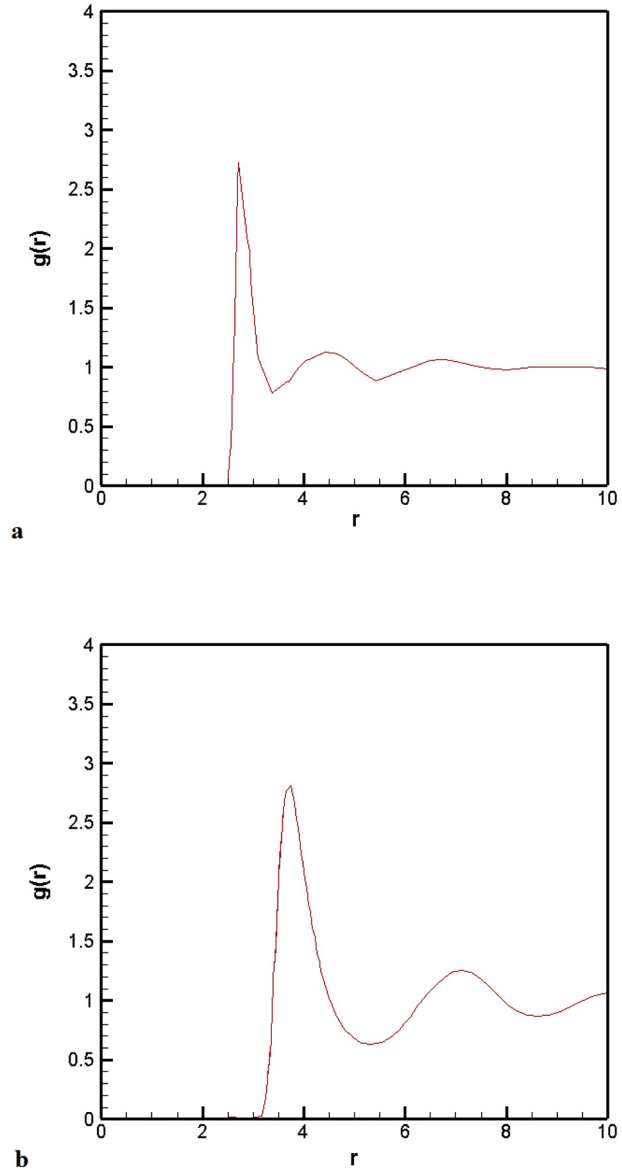

Fig. 4. RDF of a)Ar and b)O_2 fluid in Pt micro-channel in final step of DPD simulation.

in these equations, r_{ij} is a unit vector in direction ($\mathbf{r_i}$ - $\mathbf{r_j}$), $\mathbf{v_{ij}}$ is the vector difference in velocities of the two atoms ($\mathbf{v_i}$ - $\mathbf{v_j}$), α is a Gaussian random number with zero mean and unit variance, Δt is the simulation time step, and ω is a weighting parameter ($0 < \omega < 1$). Further, σ is set equal to $(2K_bT\gamma)^{1/2}$, where K_b is the Boltzmann constant and T is the temperature parameter. After determining particles interaction, DPD simulation process was fulfilled.

Further, as described by Español and Warren [22], the coefficients and the weight functions are predicted as,

$$w^D(r) = \left[w^R(r)\right]^2 \tag{6}$$

$$\gamma = \frac{\sigma^2}{2k_BT} \tag{7}$$

As required by the fluctuation-dissipation theorem. Moreover k_B is the Boltzmann constant. All of the interaction energies are expressed in units of k_BT, which is usually assigned a value of unity. One simple, straightforward and commonly used choice is,

$$w^D(r) = \left[w^R(r)\right]^2 = \left(1-\frac{r}{r_c}\right)^s \quad r < r_c \tag{8}$$

where r_c is the cut-off distance of the dissipative and random force. In DPD formulation, it usually takes the same value as the cut-off distance of the conservative force, but can vary to modify the dynamic properties in DPD simulation. The time integration algorithm is very important in DPD simulations. In order to achieve this aim, modified version of the velocity-Verlet algorithm is common,

$$r_i(t+\Delta t) = r_i(t) + \Delta t v_i(t) + \frac{1}{2}(\Delta t)^2 f_i(t) \tag{9}$$

$$v_i(t+\Delta t) + \lambda \Delta t f_i(t) \tag{10}$$

$$f_i(t+\Delta t) = f_i(r_i(t+\Delta t), v_i(t+\Delta t)) \tag{11}$$

$$v_i(t+\Delta t) = v_i(t) + \frac{1}{2}\Delta t(f_i(t) + f_i(t+\Delta t)) \tag{12}$$

In this work our DPD simulations done by using Large Scale Atomic Molecular Massively Simulator (LAMMPS) [35–37]. Fig. 1a show the schematic of Ar fluid and Pt micro-channel arrangement in first step of DPD simulations. Further, Fig. 1b represent the external magnetic field implementing to simulation systems. Technically, these graphical representations produced with OVITO software [38]. Computationally, our coarse graining models studied in 3 main Stages:

2.1. Step A) Equilibration of Ar/O_2 fluid and Pt Micro-Channel Structures

In this stage, Ar/O_2 fluid and Pt micro-channel were simulated in 1000 × 350 × 1000 box. $T = 300$ value choose as initial temperature in simulated mixtures. After this procedure, consistency of simulated structures reported by temperature and total energy calculation.

2.2. Step B) Atomic behavior of Fluid and Micro-Channel

In the second stage, by inserting external force to Ar or O_2 particles and poiseuille flow of Ar and O_2 particles the profiles of velocity, temperature and density of simulated fluid, were reported.

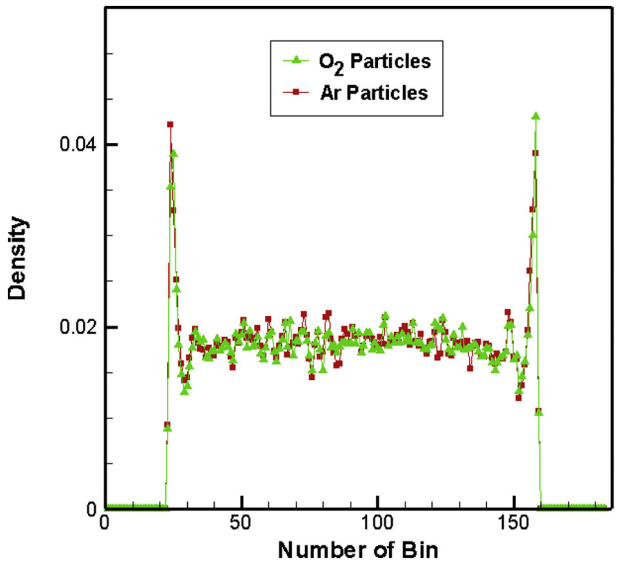

Fig. 5. Profiles of density of Ar and O_2 particles in Pt micro-channel after 1,000,000 time steps.

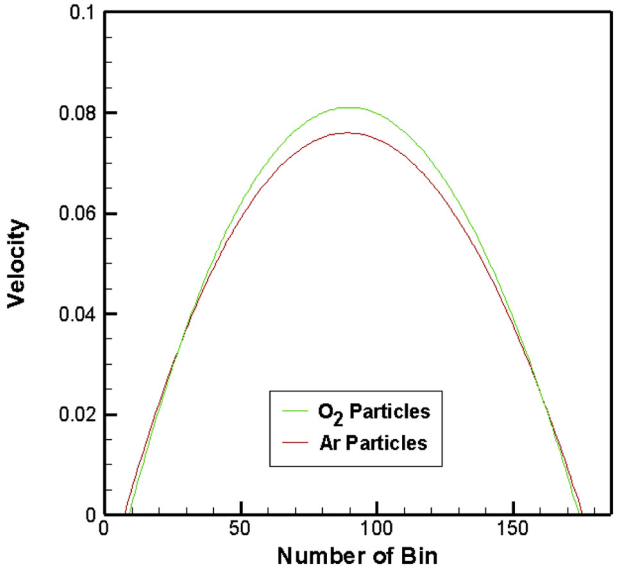

Fig. 6. Profile of Velocity of Ar and O_2 particles in Pt micro-channel after 1,000,000 time steps.

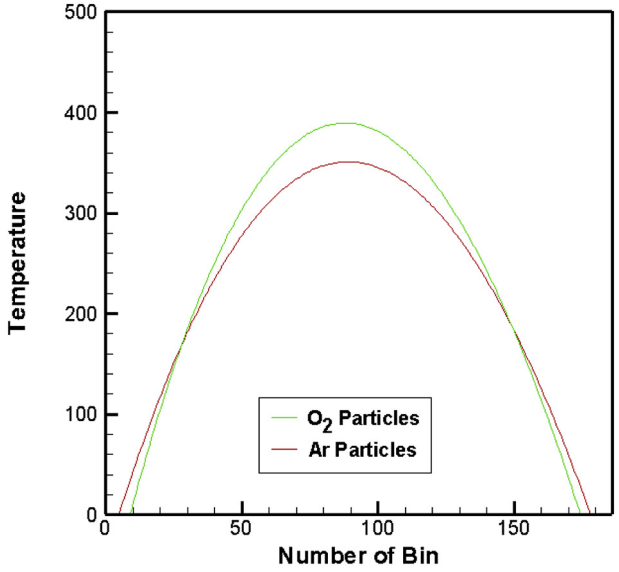

Fig. 7. Profile of temperature of Ar and O_2 particles in Pt micro-channel after 1,000,000 time steps.

2.3. Step C) External magnetic field effect on O_2/Ar particles behavior

In the final stage, by inserting external magnetic field, profiles of velocity, density and temperature variations of simulated particles were reported. The dynamic behavior of the simulated fluids in micro-channel was also expressed.

3. Results and discussion

3.1. Equilibration of Ar/O_2 and Pt Micro-Channel structures for the validation

In the first step of our DPD simulations, the consistency of simulated structures by temperature and total energy calculations, reported. In this study, $T = 300$ selected for initial temperature value for Pt micro-channel and Ar/O_2 fluid. As depicted in Fig. 2, this initial condition detectable after 2,500,000 time steps. From this calculation we can say, the mobility of simulated structures converge to constant value and temperature fluctuation vanishes by simulation time steps goes on. Fig. 3 show the total energy variation in simulated structures (fluid and micro-channel particles). This physical parameter equal to sum of potential and kinetic energies of particles. Our simulations show the total energy of O_2 and Ar fluids in Pt micro-channel converge to −690 and − 652, respectively. Physically, the negative value of total energy show the atomic consistency of them. This behavior arises from attraction force between various structures. Table 1 shows the total energy of O_2 and Ar fluids after 2,500,000 time steps. These numerical results show O_2 particles has larger value (magnitude) rather Ar fluid. By increment of total energy of simulated particles, the consistency of particles increases and so O_2 particles in Pt micro-channel has the best consistency between simulated structures with DPD approach.

Table 2
The maximum amount of temperature, density and velocity and profiles of Ar and O_2 particles in Pt micro-channel after 1,000,000 time steps.

Fluid Type	Maximum value of density (Unit Less)	Maximum value of velocity (Unit Less)	Maximum value of temperature (Unit Less)
Ar fluid	0.042	0.076	354
O_2 fluid	0.043	0.084	425

Finally, the Radial Distribution Function (RDF) of simulated structures reported to verify our simulation method. In statistical mechanics, the RDF in a system of particles, describes how density varies as a function of distance from a reference particle. Fig. 4 shows this physical parameter of Ar and O_2 particles. This calculated parameter for these particles correspond to previous report [39,40]. Physically, these calculated results show the validity of our DPD simulations which arises from appropriate atomic modeling and inter-particle force implementing in simulation box.

3.2. Atomic behavior of fluid and Micro-Channel structures

After equilibrium process, external force inserted to Ar/O_2 particles inside Pt micro-channel. After this procedure, the density, velocity and temperature profiles of fluid particles reported. For calculation of these physical quantities in our DPD simulations, we divided micro-channel to 183 bins in x direction and report the time averaging rate of temperature, density and velocity and. The density profile of Ar/O_2 fluid indicate that, particles interacted with the Pt atoms (micro-channel wall) by attraction force. Comparatively, O_2 particles attracted with larger force rather to Ar particles in Pt micro-channel. This behavior cause the maximum value of density profile reach to 0.042 and 0.043 for O_2 and Ar particles, respectively. Numerically, this maximum density rate detectable in 24/25 bin for O_2/Ar fluid. Fig. 5 show the density profile of Ar and O_2 particles in Pt micro-channel after 1,000,000 time steps. From this figure can be deduced that, the Ar/O_2 atoms absorbed by micro-channel walls and this phenomenon reduced in middle region of simulation box and particles move freely in this region. So, DPD

Table 3
Total energy of Ar/O_2 fluid in Pt micro-channel by inserting magnetic field as a function of amplitude and frequency of external field.

External Magnetic Field Type	Ar Fluid	O_2 Fluid
$B_0 = 1$	−552	−690
$B_0 = 2$	−552	−690
$B_0 = 5$	−551	−692
$\omega = 0.1$	−552	−690
$\omega = 0.2$	−553	−690
$\omega = 0.5$	−551	−691

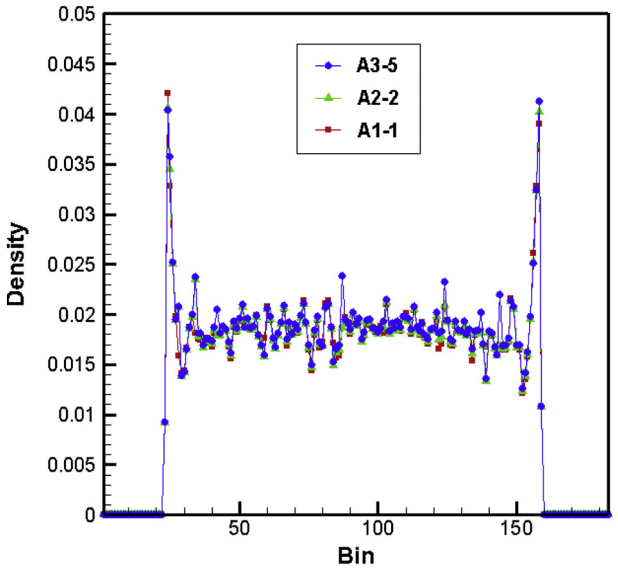

Fig. 8. Profiles of density of Ar particles in Pt micro-channel in presence of external magnetic field (various amplitudes).

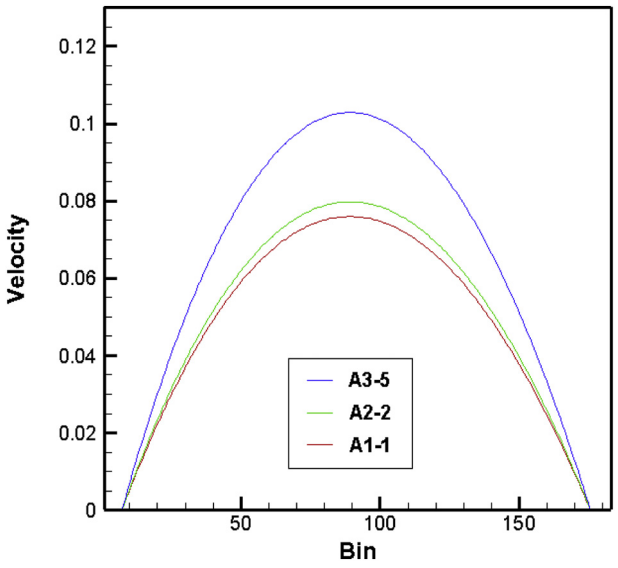

Fig. 10. Profiles of velocity of Ar particles in Pt micro-channel in presence of external magnetic field (various amplitudes).

simulations estimate poiseuille flow for Ar and O_2 particles in metallic micro-channel. This atomic calculations is Compatible with previous studies and validates our simulation method settings such as atomic modeling and interaction forces [41–51].

The velocity and temperature variations in various region of simulation box are determinant parameters in DPD simulations. In this step of our study, velocity and temperature profiles of Ar and O_2 particles reported. These profiles show the particles dynamical manner inside metallic micro-channel s. Fig. 6 shows the velocity of Ar and O_2 particles after 1,000,000 time steps. From this simulation result, we conclude the DPD approach estimate poiseuille flow for these particles in presence of external constant force.

This atomic behavior occurs because of attraction force across Pt atoms and fluid particles. In simulation box, the velocity of fluid particles in vicinity of micro-channel walls has minimum rate. Further, in middle region this physical parameter reach to maximum value. This dynamical behavior arises from 2 main factors:

1) Attraction force reach to minimum value from the Pt walls in middle region.
2) External force reach to maximum value in middle region.

Numerically, the maximum value of Ar and O_2 fluid particles occur in 83 bin of simulation box with 0.076 and 0.084, respectively. Table 2 show the maximum value of Ar and O_2 particles velocity in Pt micro-channel. Temperature fluctuation of fluid particles similar to velocity profile. Fig. 7 shows profile of temperature of Ar and O_2 particles in Pt micro-channel s after 1,000,000 time step. As illustrated in this figure, the poiseuille flow has a quadratic temperature profile. Numerically, maximum Ar and O_2 particles temperature reach to 355 and 426, respectively. These maximum values of fluid particles detectable in 88 bin. In comparison, O_2 particles temperature has bigger value rather to Ar fluid which this behavior arises from atomic weight of these structures. We can say that, Ar particles with lesser atomic mass, accelerate with larger ratio in the presence of a constant external force. In

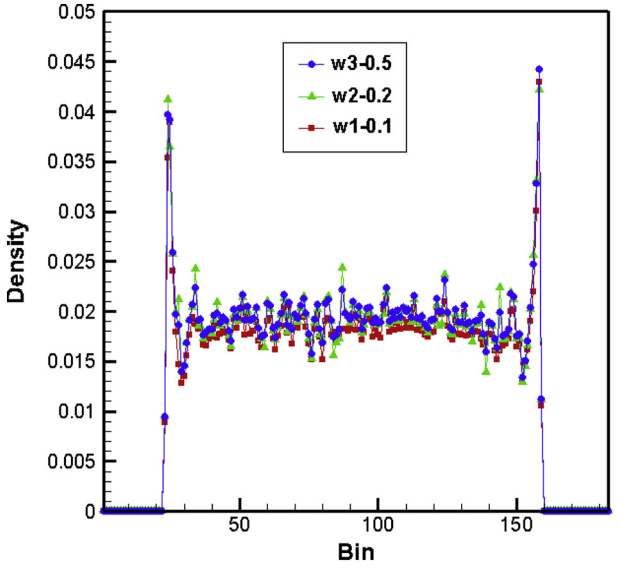

Fig. 9. Profiles of density of O_2 particles in Pt micro-channel in presence of external magnetic field (various amplitudes).

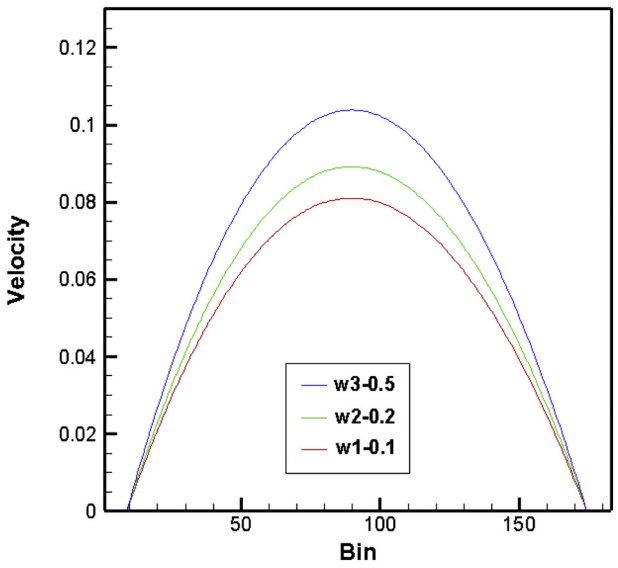

Fig. 11. Profiles of velocity of O2 particles in Pt micro-channel in presence of external magnetic field (various amplitudes).

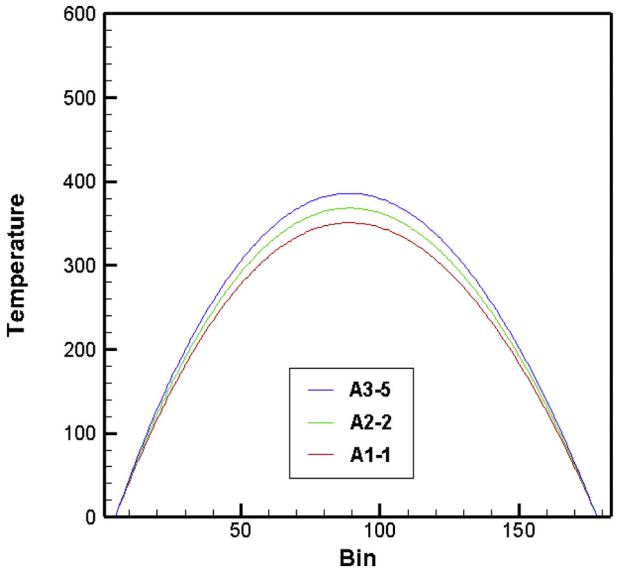

Fig. 12. Profiles of temperature of Ar particles in Pt micro-channel in presence of external magnetic field (various amplitudes).

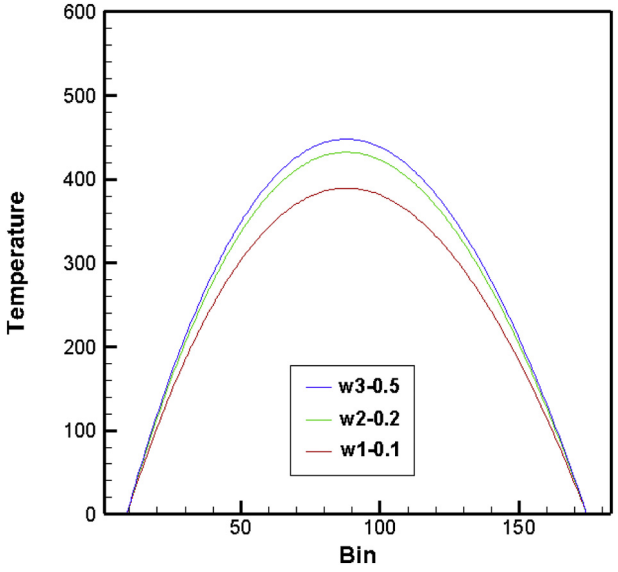

Fig. 13. Profiles of temperature of O2 particles in Pt micro-channel in presence of external magnetic field (various amplitudes).

Table 2, the maximum values of density, velocity and temperature for Ar and O_2 fluids reported after 1,000,000 time step.

3.3. External magnetic field effect on O_2/Ar particles behavior

In this section of DPD simulations, we implemented external magnetic field as below equation for the first time [52–65]:

$B=B_0 \sin(\omega t)$ (13).

This equation varies by simulation time steps. B_0 is field magnitude and ω is the frequency of this external parameter. In our DPD simulation, these physical parameters set to below values:

- $B_0 = 1$, 2, and 5
- $\omega = 0.1$, 0.2, and 0.5

As reported before, atomic consistency of simulated Ar /O_2 in Pt micro-channels reported by temperature and total energy variations as a function of simulation time steps. Our DPD simulations show the temperature of simulated structures converge to 300 after 2,500,000 time steps. Further, total energy value of simulated particles in presence of Ar/O_2 particles as fluid in Pt micro-channel reach to −553/−692 in presence of $B = 1 \times \sin(0.1 \times t)$. This atomic behavior of structures show the consistency of them in presence of external magnetic field. The total energy variation as a function of external magnetic field magnitude and frequency variation reported in Table 3. From these calculations we conclude, external magnetic field, don't disrupted atomic structures and stable phase of Ar and O_2 particles in Pt micro-channel detectable after 2,500,000 time step.

By inserting external magnetic field, the poissue flow of Ar/O_2 particles can be seen. From Figs. 8 and 9, we see density value reach to maximum value in initial and final bins of simulated structures. Further, density profile fluctuate with mean value in middle region of simulation box which this behavior arises from external parameters (external force and external magnetic field). Numerically, the maximum density of simulated fluids reach to 0.042 and 0.043 for Ar and O_2 particles. So, we can say this atomic parameter increases 71% and 73% for simulated fluids (Ar and O_2, respectively). Velocity profile of simulated particles get bigger value by magnetic field implementing in simulation box. For $B_0 = 1$ and $\omega = 0.1$ values, the maximum rate of particles velocity reach to 0.104/0.108 for Ar/O_2 fluid (see Figs. 10 and 11). This maximum value of calculated quantity occur in middle bins of simulation box. In comparison, O_2 fluid reach larger atomic velocity which these atomic manner arises from charge distribution and lesser atomic mass of this element. As depicted in Figs. 12 and 13, by velocity increasing in simulated structures, temperature value increases, too. In 88 bin of simulated fluids with Ar and O_2 particles, the maximum ratio of temperatures detected with 390 and 489 values (for $B_0 = 1$). Numerically, by amplitude of external magnetic field increasing, the density (maximum value), velocity and temperature profiles increased. The maximum rate of these physical quantities in presence of external magnetic field with ($B_0 =$ 1, 2, and 5) reported in Table 4.

Frequency (ω) of external magnetic field variation show the similar effect which described for amplitude study with less intensity. By increasing ω form 0.1 to 0.5 values, the maximum rate of density profile reach to 0.042 and 0.043 for Ar and O_2 fluids. This atomic behavior show that, distracting force implemented to fluid particles and distribution of theses structure increases in vicinity of micro-channel walls. By this particle distribution, free space for fluid particles increases and Ar/O_2 fluid movement by larger velocity in middle of micro-channel. Table 5 show the maximum ratio of Ar and O_2 particles velocity reach to 0.095 and 0.101 values, respectively. This maximum ratio, detected in middle bins of simulation box. Further, temperature profile of simulated structures follow of similar behavior and maximum ratio of this physical quantity reach to 374 and 452 values for Ar and O_2 particles

Table 4
The maximum rate of O_2/Ar fluid density, velocity and temperature profiles in Pt micro-channel s as a function of external magnetic field by various amplitudes.

Sample	Maximum Value of Density	Maximum Value of Velocity	Maximum Value of Temperature
Ar particles – $B_0 = 1$	0.041	0.076	354
Ar particles – $B_0 = 2$	0.042	0.080	372
Ar particles – $B_0 = 5$	0.042	0.104	390
O_2 particles – $B_0 = 1$	0.042	0.084	425
O_2 particles – $B_0 = 2$	0.042	0.093	472
O_2 particles – $B_0 = 5$	0.043	0.108	489

Table 5
The maximum rate of O_2/Ar fluid density, velocity and temperature profiles in Pt micro-channel s as a function of external magnetic field by various frequencies.

Sample	Maximum Value of Density	Maximum Value of Velocity	Maximum Value of Temperature
Ar particles – $\omega = 0.1$	0.041	0.076	354
Ar particles – $\omega = 0.2$	0.041	0.078	361
Ar particles – $\omega = 0.5$	0.042	0.095	374
O_2 particles – $\omega = 0.1$	0.042	0.084	425
O_2 particles – $\omega = 0.2$	0.042	0.088	431
O_2 particles – $\omega = 0.5$	0.043	0.101	452

by external magnetic field with $\omega = 0.5$, respectively. By these calculated results, we conclude frequency variation of external magnetic field don't disturbed the fluid behavior and can be used in industrial applications for heat and mass transfer procedures.

4. Conclusion

In this work, we use dissipative particle dynamics (DPD) simulations to describe the external magnetic field (time dependent) effects on behavior of Ar and O_2 particles in Pt micro-channel. In our calculations, magnetic field with various magnitude and frequencies implemented to simulation box in perpendicular to fluid direction. Our DPD simulations results show that, this external field is an important parameter to Ar and O_2 particles behavior. Numerically, our calculated results from DPD computational process as follow:

A. The temperature of simulated structures equilibrated in 300 value by implementing of external magnetic field.
B. The potential energy of simulated structures reach to −552/−690 value for Ar/O_2 particles by implementing of external magnetic field.
C. By external magnetic field inserting to Ar and O_2 particles, the maximum value of these structures density reach to 0.042 and 0.043 value.
D. Maximum rate of velocity profile calculated for Ar/O_2 particles by $B_0 = 5$ and $w = 0.5$ magnetic field with 0.104/0.108 values.
E. Temperature of simulated fluid particles reach to 390 and 489 for Ar and O_2 fluids by implementing of external magnetic field in DPD simulations.

Finally, these results of our DPD study with LAMMPS package show that, one can be used external magnetic field in various industrial process such as mass and heat transfer procedures to increase their efficiency.

Declaration of Competing Interest

There is no conflict of interest.

References

[1] Robert Byron Bird, Warren E. Stewart, Edward N. Lightfoot, Transport Phenomena, Revised Second ed. Wiley, New York, 2007 912 ISBN 0-471-41077-2.
[2] Michael Eckert, The Dawn of Fluid Dynamics: A Discipline between Science and Technology, Wiley, 2006 ix ISBN 3-527-40513-5.
[3] J.D. Anderson, Fundamentals of Aerodynamics, 4th ed. McGraw–Hill, London, 2007 ISBN 0-07-125408-0.
[4] Nishant Nangia, Hans Johansen, Neelesh A. Patankar, Amneet Pal S. Bhalla, A moving control volume approach to computing hydrodynamic forces and torques on immersed bodies, J. Comput. Phys. 347 (2017) 437–462 arXiv:1704.00239 , Bibcode: 2017JCoPh.347..437N https://doi.org/10.1016/j.jcp.2017.06.047.
[5] Robert Fox, Alan McDonald, Philip Pritchard, Fluid Mechanics, 8 ed. John Wiley & Sons., 2012 76–83 ISBN 978-1-118-02641-0.
[6] M.R. Salimpour, A.T. Al-Sammarraie, A. Forouzandeh, M. Farzaneh, Constructal design of circular multilayer micro-channel heat sinks, J. Thermal. Sci. Eng. Appl. 11 (1) (2019), 011001, https://doi.org/10.1115/1.4041196.
[7] D.B. Tuckerman, R.F.W. Pease, High-performance heat sinking for VLSI, IEEE Elect. Dev. Lett. 2 (5) (1981) 126–129, https://doi.org/10.1109/EDL.1981.25367.
[8] Satish G. Kandlikar, Heat Transfer and Fluid Flow in Minichannels and Micro-Channel S, Elsevier B.V, Amsterdam, The Netherlands, 2006 450 ISBN 978-0-08-044527-4.
[9] Martin S. Silberberg, Chemistry: The Molecular Nature of Matter and Change, McGraw-Hill Higher Education, 2009 448–449 ISBN 978-0-07-304859-8.
[10] R. Sabetvand, M.E. Ghazi, M. Izadifard, DFT study of electronic and optical properties of CH3NH3SnI3 perovskite, Energy Sourc. Part A: Recov. Utiliz. Environ. Effects (2020) 1–13, https://doi.org/10.1080/15567036.2020.1805047.
[11] A. Karimipour, N.A. Jolfaei, M. Hekmatifar, D. Toghraie, R. Sabetvand, A. Karimipour, Prediction of the interaction between HIV viruses and human serum albumin (HSA) molecules using an equilibrium dynamics simulation program for application in bio medical science, J. Mol. Liq. (2020) 113989, https://doi.org/10.1016/j.molliq.2020.113989.
[12] A. Ghanbari, F. Warchomicka, C. Sommitsch, A. Zamanian, Investigation of the oxidation mechanism of dopamine functionalization in an AZ31 magnesium alloy for biomedical applications, Coatings 9 (9) (2019) 584, https://doi.org/10.3390/coatings9090584.
[13] M.H. Nafar Sefiddashti, M. Boudaghi-Khajehnobar, B.J. Edwards, B. Khomami, High-fidelity scaling relationships for determining dissipative particle dynamics parameters from atomistic molecular dynamics simulations of polymeric liquids, Sci. Rep. 10 (1) (2020)https://doi.org/10.1038/s41598-020-61374-8.
[14] Q. Shao, S. Matthai, T. Driesner, L. Gross, Predicting plume spreading during CO2 geo-sequestration: benchmarking a new hybrid finite element–finite volume compositional simulator with asynchronous time marching, Comput. Geosci. (2020) https://doi.org/10.1007/s10596-020-10006-1.
[15] Y. Zheng, X. Zhang, M.T. Soleimani Mobareke, M. Hekmatifar, A. Karimipour, R. Sabetvand, Potential energy and atomic consistency of H2O/CuO nanoparticles flow and heat transfer in non-ideal micro-channel via molecular dynamic approach: the green–Kubo method, J. Therm. Anal. Calorim. (2020)https://doi.org/10.1007/s10973-020-10054-w.
[16] Y. Zheng, X. Zhang, M. Nouri, A. Amini, A. Karimipour, M. Hekmatifar, ... A. Karimipour, Atomic rheology analysis of the external magnetic field effects on nanofluid in non-ideal micro-channel via molecular dynamic method, Journal of Thermal Analysis and Calorimetry. (2020) https://doi.org/10.1007/s10973-020-10191-2.
[17] A. Asgari, Q. Nguyen, A. Karimipour, Q.-V. Bach, M. Hekmatifar, R. Sabetvand, Investigation of additives nanoparticles and sphere barriers effects on the fluid flow inside a nanochannel impressed by an extrinsic electric field: a molecular dynamics simulation, J. Mol. Liq. (2020), 114023, https://doi.org/10.1016/j.molliq.2020.114023.
[18] A. Mosavi, M. Hekmatifar, A. Alizadeh, D. Toghraie, R. Sabetvand, A. Karimipour, The molecular dynamics simulation of thermal manner of Ar/Cu nanofluid flow: the effects of spherical barriers size, J. Mol. Liq. 114183 (2020) https://doi.org/10.1016/j.molliq.2020.114183.
[19] H. Chen, Q. Nie, H. Fang, Many-body dissipative particle dynamics simulation of Newtonian and non-Newtonian nanodroplets spreading upon flat and textured substrates, Appl. Surf. Sci. 519 (2020) 146250, https://doi.org/10.1016/j.apsusc.2020.146250.
[20] R. Zakeri, M. Sabouri, A. Maleki, Z. Abdelmalek, Investigation of magneto hydrodynamics effects on a polymer chain transfer in Micro-Channel using dissipative particle dynamics method, Symmetry 12 (3) (2020) 397, https://doi.org/10.3390/sym12030397.
[21] P.J. Hoogerbrugge, J.M.V.A. Koelman, Simulating microscopic hydrodynamic phenomena with dissipative particle dynamics, Europhys. Lett. (EPL) 19 (3) (1992) 155–160 , Bibcode:1992EL.....19..155H https://doi.org/10.1209/0295-5075/19/3/001 (ISSN 0295-5075).
[22] P. Español, P. Warren, Statistical mechanics of dissipative particle dynamics, Europhys. Lett. (EPL) 30 (4) (1995) 191–196 , Bibcode:1995EL....30..191E https://doi.org/10.1209/0295-5075/30/4/001 ISSN 0295-5075. S2CID 14385201.
[23] Emad Moeendarbary, Teng Yong Ng, M. Zangeneh, Dissipative particle dynamics: introduction, methodology and complex fluid applications - a review, Int. J. Appl. Mech. 1 (4) (2009) 737–763 , Bibcode:2009IJAM....1..737M https://doi.org/10.1142/S1758825109000381 S2CID 50363270.
[24] Sebastian Kmiecik, Dominik Gront, Michal Kolinski, Lukasz Wieteska, Aleksandra Elzbieta Dawid, Andrzej Kolinski, Coarse-grained protein models and their applications, Chem. Rev. 116 (14) (2016-06-22) 7898–7936, https://doi.org/10.1021/acs.chemrev.6b00163 ISSN 0009-2665. PMID 27333362.
[25] Helgi I. Ingólfsson, Cesar A. Lopez, Jaakko J. Uusitalo, Djurre H. de Jong, Srinivasa M. Gopal, Xavier Periole, Siewert J. Marrink, The power of coarse graining in biomolecular simulations, Wiley Interdiscipl. Rev.: Computat. Mol. Sci. 4 (3) (2014-05-01)

225–248, https://doi.org/10.1002/wcms.1169 ISSN 1759-0884. PMC 4171755. PMID 25309628.
[26] Riccardo Baron, Daniel Trzesniak, Alex H. de Vries, Andreas Elsener, Siewert J. Marrink, Wilfred F. van Gunsteren, Comparison of thermodynamic properties of coarse-grained and atomic-level simulation models, ChemPhysChem. 8 (3) (2007-02-19) 452–461, https://doi.org/10.1002/cphc.200600658 ISSN 1439-7641. PMID 17290360.
[27] Z. Xu, Y. Yang, G. Zhu, P. Chen, Z. Huang, X. Dai, ... L.-T. Yan, Simulating transport of soft matter in micro/nano channel flows with dissipative particle dynamics, Adv. Theory Simul. (2018), 1800160, https://doi.org/10.1002/adts.201800160.
[28] E. Abu-Nada, I. Pop, O. Mahian, A dissipative particle dynamics two-component nanofluid heat transfer model: application to natural convection, Int. J. Heat Mass Transf. 133 (2019) 1086–1098, https://doi.org/10.1016/j.ijheatmasstransfer.2018.12.151.
[29] Z. Tong, H. Liu, Y. Liu, H. Li, S. Jiang, J. Chang, ... H. Hao, A study on the dynamic behavior of macromolecular suspension flow in micro-channel under thermal gradient using energy-conserving dissipative particle dynamics simulation, Microfluidics and Nanofluidics 24 (5) (2020) https://doi.org/10.1007/s10404-020-02338-2.
[30] N. Mai-Duy, T.Y.N. Nguyen, K. Le-Cao, N. Phan-Thien, Investigation of particulate suspensions in generalised hydrodynamic dissipative particle dynamics using a spring model, Appl. Math. Model. (2019) https://doi.org/10.1016/j.apm.2019.07.065.
[31] P.J. Hoogerbrugge, J.M.V.A. Koelman, Simulating microscopic hydrodynamic phenomena with dissipative particle dynamics, Europhys. Lett. (EPL). 19 (3) (1992) 155–160 , Bibcode:1992EL.....19..155H https://doi.org/10.1209/0295-5075/19/3/001 (ISSN 0295-5075).
[32] J.M.V.A. Koelman, P.J. Hoogerbrugge, Dynamic simulations of hard-sphere suspensions under steady shear, Europhys. Lett. (EPL). 21 (3) (1993) 363–368 , Bibcode:1993EL.....21..363K. https://doi.org/10.1209/0295-5075/21/3/018 (ISSN 0295-5075).
[33] P. Español, P. Warren, Statistical mechanics of dissipative particle dynamics, Europhys. Lett. (EPL). 30 (4) (1995) 191–196, s https://doi.org/10.1209/0295-5075/30/4/001 (ISSN 0295-5075).
[34] N. Goga, A.J. Rzepiela, A.H. de Vries, S.J. Marrink, H.J.C. Berendsen, Efficient algorithms for Langevin and DPD dynamics, J. Chem. Theory Comput. 8 (10) (2012) 3637–3649, https://doi.org/10.1021/ct3000876 ISSN 1549-9618. PMID 26593009.
[35] S.J. Plimpton, A.P. Thompson, Computational aspects of many-body potentials, MRS Bull. 37 (05) (2012) 513–521, https://doi.org/10.1557/mrs.2012.96.
[36] W.M. Brown, P. Wang, S.J. Plimpton, A.N. Tharrington, Implementing molecular dynamics on hybrid high performance computers – short range forces, Comput. Phys. Commun. 182 (4) (2011) 898–911, https://doi.org/10.1016/j.cpc.2010.12.021.
[37] W.M. Brown, A. Kohlmeyer, S.J. Plimpton, A.N. Tharrington, Implementing molecular dynamics on hybrid high performance computers – particle–particle particle-mesh, Comput. Phys. Commun. 183 (3) (2012) 449–459, https://doi.org/10.1016/j.cpc.2011.10.012.
[38] A. Stukowski, Visualization and analysis of atomistic simulation data with OVITO–the open visualization tool, Model. Simul. Mater. Sci. Eng. 18 (1) (2009) 015012, https://doi.org/10.1088/0965-0393/18/1/015012.
[39] A.P. Jones, J. Crain, V.P. Sokhan, T.W. Whitfield, G.J. Martyna, Quantum Drude oscillator model of atoms and molecules: many-body polarization and dispersion interactions for atomistic simulation, Phys. Rev. B 87 (14) (2013) https://doi.org/10.1103/physrevb.87.144103.
[40] A.P. Jones, J. Crain, V.P. Sokhan, T.W. Whitfield, G.J. Martyna, Quantum Drude oscillator model of atoms and molecules: many-body polarization and dispersion interactions for atomistic simulation, Phys. Rev. B 87 (14) (2013) https://doi.org/10.1103/physrevb.87.144103.
[41] E.E. Keaveny, I.V. Pivkin, M. Maxey, G. Em Karniadakis, A comparative study between dissipative particle dynamics and molecular dynamics for simple- and complex-geometry flows, J. Chem. Phys. 123 (10) (2005) 104107, https://doi.org/10.1063/1.2018635.
[42] Shao-Feng Xu, Jiu-Gen Wang, Dissipative particle dynamics simulation of macromolecular solutions under Poiseuille flow in micro-channels, Acta Phys. Sin. 62 (12) (2013) 124701, https://doi.org/10.7498/aps.62.124701.
[43] A. Taghipour, A. Karimipour, M. Afrand, S. Yaghoubi, M. Akbari, Develop dissipative particle dynamics method to study the fluid flow and heat transfer of Ar and O2 flows in the micro- and nanochannels with precise atomic arrangement versus molecular dynamics approach, J. Therm. Anal. Calorim. (2020) https://doi.org/10.1007/s10973-020-10329-2.
[44] M.R. Safaei, M. Safdari Shadloo, M.S. Goodarzi, A. Hadjadj, H.R. Goshayeshi, M. Afrand, S.N. Kazi, A survey on experimental and numerical studies of convection heat transfer of nanofluids inside closed conduits, Adv. Mech. Eng. 8 (10) (2016) p.1687814016673569.
[45] H.R. Goshayeshi, M.R. Safaei, M. Goodarzi, M. Dahari, Particle size and type effects on heat transfer enhancement of Ferro-nanofluids in a pulsating heat pipe, Powder Technol. 301 (2016) 1218–1226.
[46] H.R. Goshayeshi, M. Goodarzi, M. Dahari, Effect of magnetic field on the heat transfer rate of kerosene/Fe2O3 nanofluid in a copper oscillating heat pipe, Exp. Thermal Fluid Sci. 68 (2015) 663–668.
[47] H. Mahdisoozani, M. Mohsenizadeh, M. Bahiraei, A. Kasaeian, A. Daneshvar, M. Goodarzi, M.R. Safaei, Performance enhancement of internal combustion engines through vibration control: state of the art and challenges, Appl. Sci. 9 (3) (2019) 406.
[48] Z. Li, M.M. Sarafraz, A. Mazinani, T. Hayat, H. Alsulami, M. Goodarzi, Pool boiling heat transfer to CuO-H2O nanofluid on finned surfaces, Int. J. Heat Mass Transf. 156 (2020) 119780.
[49] Z. Li, A. Mazinani, T. Hayat, A.A. Al-Rashed, H. Alsulami, M. Goodarzi, M.M. Sarafraz, Transient pool boiling and particulate deposition of copper oxide nano-suspensions, Int. J. Heat Mass Transf. 155 (2020) 119743.
[50] M.R. Safaei, I. Tlili, E. Gholamalizadeh, T. Abbas, T.A. Alkanhal, M. Goodarzi, M. Dahari, Thermal analysis of a binary base fluid in pool boiling system of glycol–water alumina nano-suspension, J. Therm. Anal. Calorim. (2020) 1–10.
[51] A.A. Ahmadi, M. Arabbeiki, H.M. Ali, M. Goodarzi, M.R. Safaei, Configuration and optimization of a minichannel using water–alumina nanofluid by non-dominated sorting genetic algorithm and response surface method, Nanomaterials 10 (5) (2020) 901.
[52] T. Abdulrazzaq, H. Togun, M. Goodarzi, S.N. Kazi, M.K.A. Ariffin, N.M. Adam, K. Hooman, Turbulent heat transfer and nanofluid flow in an annular cylinder with sudden reduction, J. Therm. Anal. Calorim. (2020) 1–13.
[53] M.N.H. Mat, N.Z. Asmuin, M.F.M. Basir, M. Goodarzi, M.F. Abd Rahman, R. Khairulfuaad, B.A. Jabbar, M.S.M. Kasihmuddin, Influence of divergent length on the gas-particle flow in dual hose dry ice blasting nozzle geometry, Powder Technol. 364 (2020) 152–158.
[54] H. Arasteh, R. Mashayekhi, M. Goodarzi, S.H. Motaharpour, M. Dahari, D. Toghraie, Heat and fluid flow analysis of metal foam embedded in a double-layered sinusoidal heat sink under local thermal non-equilibrium condition using nanofluid, J. Therm. Anal. Calorim. 138 (2) (2019) 1461–1476.
[55] M.H. Nadimi-Shahraki, et al., MTDE: An effective multi-trial vector-based differential evolution algorithm and its applications for engineering design problems, Appl. Soft Comput. 14 (2020) 106761.
[56] M.H. Nadimi-Shahraki, S. Taghian, S. Mirjalili, An improved grey wolf optimizer for solving engineering problems, Expert Syst. Appl. (2020) 113917.
[57] Hoda Zamani, Mohammad H. Nadimi-Shahraki, Amir H. Gandomi, CCSA: conscious neighborhood-based crow search algorithm for solving global optimization problems, Appl. Soft Comput. 85 (2019), 105583.1, .
[58] Hoda Zamani, Mohammad Hossein Nadimi-Shahraki, Swarm intelligence approach for breast Cancer diagnosis, Int. J. Comput. Appl. 151 (1) (2016) 40–44.
[59] Hoda Zamani, Mohammad Hossein Nadimi-Shahraki, Feature selection based on whale optimization algorithm for diseases diagnosis, Intern. J. Comput. Sci. Inform. Secur. 14 (9) (2016) 1243–1247.
[60] E. Shafigh Fard, Khalil Monfaredi, Mohammad Hossein Nadimi-Shahraki, An area-optimized chip of ant colony algorithm design in hardware platform using the address-based method, Intern. J. Elect. Comput. Eng. 4 (6) (2014) 989–998.
[61] R. Ranjbarzadeh, A. Moradikazerouni, R. Bakhtiari, A. Asadi, M. Afrand, An experimental study on stability and thermal conductivity of water/silica nanofluid: eco-friendly production of nanoparticles, J. Clean. Prod. 206 (2019) 1089–1100.
[62] R. Ranjbarzadeh, A. Akhgar, S. Musivand, M. Afrand, Effects of graphene oxide-silicon oxide hybrid nanomaterials on rheological behavior of water at various time durations and temperatures: synthesis, preparation and stability, Powder Technol. 335 (2018) 375–387.
[63] A.A. Al-Rashed, R. Ranjbarzadeh, S. Aghakhani, M. Soltanimehr, M. Afrand, T.K. Nguyen, Entropy generation of boehmite alumina nanofluid flow through a minichannel heat exchanger considering nanoparticle shape effect, Phys. A: Statist. Mech. Appl. 521 (2019) 724–736.
[64] M.R. Safaei, R. Ranjbarzadeh, A. Hajizadeh, M. Bahiraei, M. Afrand, A. Karimipour, Effects of cobalt ferrite coated with silica nanocomposite on the thermal conductivity of an antifreeze: new nanofluid for refrigeration condensers, Int. J. Refrig. 102 (2019) 86–95.
[65] Y. Xu, Q. Nguyen, O. Malekahmadi, R. Hadi, Z. Jokar, A. Mardani, A. Karimipour, R. Ranjbarzadeh, Z. Li, Q.V. Bach, Synthesis and characterization of additive graphene oxide nanoparticles dispersed in water: experimental and theoretical viscosity prediction of non-Newtonian nanofluid, Math. Methods Appl. Sci. (2020) (in press).